

# Ethane hydrogenolysis on silica-supported tantalum hydride. Quantum-chemical study

M. N. Mikhailov,<sup>a\*</sup> A. A. Bagatur'yants,<sup>b</sup> and L. M. Kustov<sup>a</sup>

<sup>a</sup>N. D. Zelinsky Institute of Organic Chemistry, Russian Academy of Sciences,  
47 Leninsky prosp., 119991 Moscow, Russian Federation.

Fax: +7 (095) 137 2935. E-mail: mik@ioc.ac.ru

<sup>b</sup>Photochemistry Center, Russian Academy of Sciences,  
7a ul. Novatorov, 117421 Moscow, Russian Federation.

Fax: +7 (095) 936 1255. E-mail: sasha@photonics.ru

The structures of the  $(\text{H}_4\text{Si}_2\text{O}_5)\text{O}_2\text{Ta}(\text{R}, \text{RR}'\text{R}'', \text{RR}''')$  clusters ( $\text{R}, \text{R}'', \text{R}''' = \text{H}, \text{Me}, \text{Et}, \text{Pr}; \text{R}'' = \text{CH}_2$ ), which model the basic structural units of the catalytic cycle of ethane hydrogenolysis on silica-supported tantalum hydride, were studied by the density functional theory (B3LYP) and the perturbation theory (MP2). The possible structure of active sites was proposed based on comparison of experimental results with calculated data. Ethane hydrogenolysis and metathesis proceed by a mechanism involving the formation of ethylene  $\pi$ -complexes and carbenium derivatives of tantalum as intermediates.

**Key words:** alkane hydrogenolysis, C—C bond activation, C—H bond activation, tantalum complexes.

Activation of alkanes is still one of the most important problems in catalytic chemistry. In recent years, a new generation of catalysts, *viz.*, silica-supported transition metal hydrides, has attracted attention.<sup>1–17</sup> These catalysts are prepared by reactions of the corresponding organometallic compounds with partially dehydroxylated silica gel followed by reduction of the resulting surface complexes.<sup>3,8</sup>

Recently,<sup>17</sup> it has been demonstrated that silica-supported tantalum hydride exhibits activity in hydrogenolysis of  $\text{C}_3$ – $\text{C}_5$  alkanes at moderate temperatures (25–200 °C). This reaction is accompanied by the cleavage of the C—C and C—H bonds followed by the formation of lower homologs up to methane from alkanes. The feature characterizing the behavior of tantalum-based catalysts is that they exhibit catalytic activity in ethane hydrogenolysis, whereas analogous zirconium-based systems catalyze hydrogenolysis of alkanes containing three or more carbon atoms in the chain.<sup>2</sup>

The aim of the present study was to investigate the structures of the active sites and the mechanism of ethane hydrogenolysis on silica-supported tantalum hydride by quantum-chemical methods.

## Calculation procedure

All calculations were carried out by the density functional theory (DFT) using the B3LYP exchange-correlation functional and by the restricted Hartree–Fock (RHF) method with inclu-

sion of electron correlation at the second-order Möller–Plesset perturbation theory (MP2) level. To decrease the computation time, the SBK pseudopotential<sup>18</sup> and the corresponding basis set supplemented with polarization functions on all atoms were used. Calculations were carried out with full optimization of geometric parameters, unless otherwise indicated. All calculations were performed using the GAMESS(US) program package.<sup>19</sup>

## Results and Discussion

**Model and structure of active sites.** The modified silica surface was modeled with the  $(\text{H}_4\text{Si}_2\text{O}_5)(\text{OH})_2$  cluster. The latter is a fragment of the  $\text{SiO}_2$  crystal with the  $\beta$ -cristobalite structure in which the broken bonds at the cluster boundary are saturated with hydroxy groups<sup>20,21</sup> (Fig. 1, *a*, *b*). The terminal OH groups thus formed were fixed in the calculations. We chose this cluster because the structure of silica gel used in experiments on the surface modification most closely resembles the cristobalite structure with a large number of isolated terminal OH groups and also based on the experimental data<sup>8</sup> providing evidence that the Ta atom is coordinated by two O atoms.

Test calculations of large clusters demonstrated that cluster expansion has virtually no effect on the structure of the surface fragment. The replacement of the terminal H atoms of the initial  $(\text{H}_4\text{Si}_2\text{O}_5)(\text{OH})_2$  cluster by organometallic groups leads to an increase in the Si—O bond



**Fig. 1.** Structures of  $\beta$ -cristobalite (a), the cluster, which models the silica surface (b), and the optimized structure of the  $(\text{H}_4\text{Si}_2\text{O}_5)\text{O}_2\text{TaH}_3$  cluster (c) ( $\text{O}_x$  and  $\text{H}_x$  are the fixed atoms). Here and in Fig. 2, the bond lengths are given (in  $\text{\AA}$ ).

lengths in the first coordination sphere by 0.02–0.04  $\text{\AA}$ , whereas the bond lengths in the second coordination sphere remain unchanged. These facts indicate that the properties of the surface organometallic compounds are adequately modeled by small clusters.

With the aim of determining the possible structure of the active sites, we compared the calculated vibrational frequencies of the  $(\text{H}_4\text{Si}_2\text{O}_5)\text{O}_2\text{TaH}_3$  (**1**) and  $(\text{H}_4\text{Si}_2\text{O}_5)\text{O}_2\text{TaH}$  clusters with the experimental IR spectrum (Table 1). The IR spectrum has three bands in the region of  $1800 \text{ cm}^{-1}$  (at 1855, 1830, and  $1815 \text{ cm}^{-1}$ ), which were assigned<sup>8</sup> to vibrations of tantalum monohydride. However, the positions and intensities of these bands are in much better agreement with the assumption that tantalum trihydride is formed on the silica surface. Hence, tantalum trihydrides rather than tantalum monohydrides serve, most likely, as active sites.

The optimized structure of the  $(\text{H}_4\text{Si}_2\text{O}_5)\text{O}_2\text{TaH}_3$  cluster (**1**) modeling the active sites is shown in Fig. 1, c. Compared to the B3LYP method, the MP2 method predicts a somewhat larger correlation effect. However, the difference between the values calculated according to these two methods is  $\leq 0.01 \text{ \AA}$  (Table 2).

**Catalytic cycle of ethane hydrogenolysis.** The catalytic cycle of alkane hydrogenolysis is shown in Scheme 1. The key step of the catalytic cycle is  $\sigma$ -bond metathesis including intramolecular exchange, where the coordination

**Table 1.** Calculated and experimental<sup>8</sup> vibrational frequencies ( $\nu/\text{cm}^{-1}$ ) of the  $(\text{H}_4\text{Si}_2\text{O}_5)\text{O}_2\text{TaH}_3$  and  $(\text{H}_4\text{Si}_2\text{O}_5)\text{O}_2\text{TaH}$  clusters in IR spectra

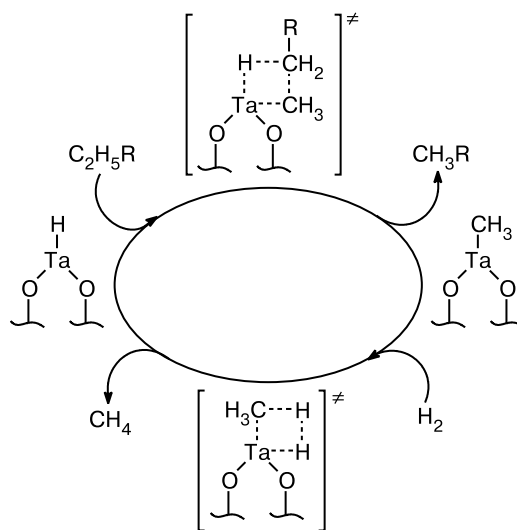
Vibration mode	Calculation		Experiment
	B3LYP	MP2	
$\nu_s(\text{TaH}_3)$	1913, 1844	1917, 1850	1855, 1815
$\nu_{as}(\text{TaH}_3)$	1864	1868	1830
$\nu_s(\text{TaD}_3)$	1358, 1305	1361, 1310	—
$\nu_{as}(\text{TaD}_3)$	1325	1328	—
$\nu(\text{TaH})$	1804	1810	—
$\nu(\text{TaD})$	1280	1284	—

**Table 2.** Calculated and experimental<sup>8</sup>  $\text{Ta}—\text{O}$  bond lengths ( $d/\text{\AA}$ )

Cluster	Calculation		Experiment
	B3LYP	MP2	
$(\text{H}_4\text{Si}_2\text{O}_5)\text{O}_2\text{TaH}_3$	1.910, 1.901	1.910, 1.907	1.893
$(\text{H}_4\text{Si}_2\text{O}_5)\text{O}_2\text{TaH}$	1.887, 1.887	1.893, 1.892	1.893

number of the metal atom (a four-center transition state) remains unchanged.<sup>17</sup> However, as we have demonstrated earlier,<sup>22</sup> the occurrence of such catalytic cycles on tantalum monohydride seems to be unlikely.

**Scheme 1**



$\text{R} = \text{H, Alk}$

We proposed the catalytic cycle of ethane hydrogenolysis based on tantalum trihydride **1** (Scheme 2). The optimized structures of the clusters, which model the main intermediates and transition states (TS) of this cycle, are shown in Fig. 2. The nature of all stationary points was confirmed based on analysis of the matrices of second

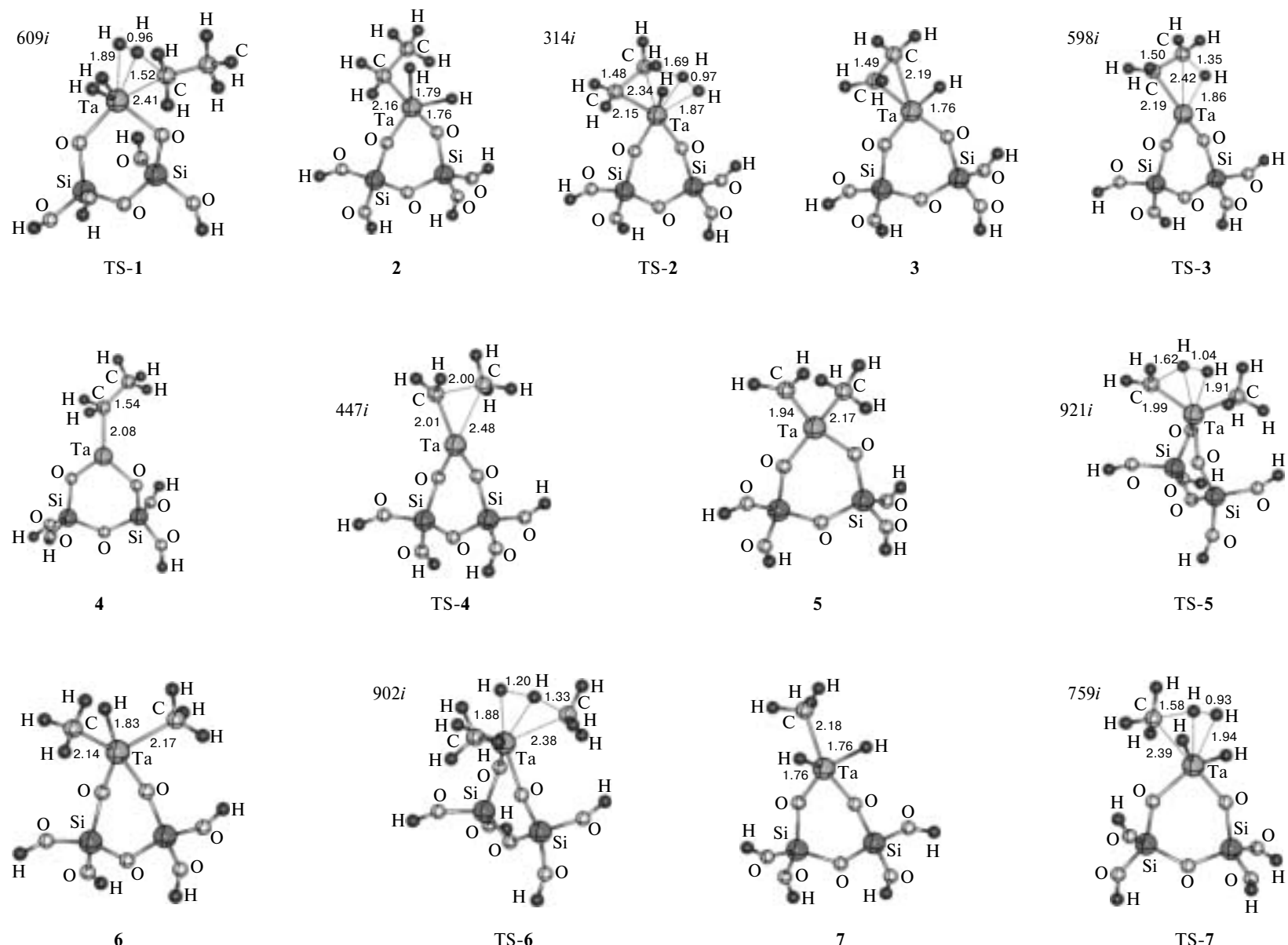


**Fig. 2.** Optimized structures of the clusters, which model the main intermediates (2–7) and transition states (TS-1–TS-7) of the catalytic cycle of ethane hydrogenolysis (for each TS, the imaginary frequency corresponding to the reaction coordinate is given).

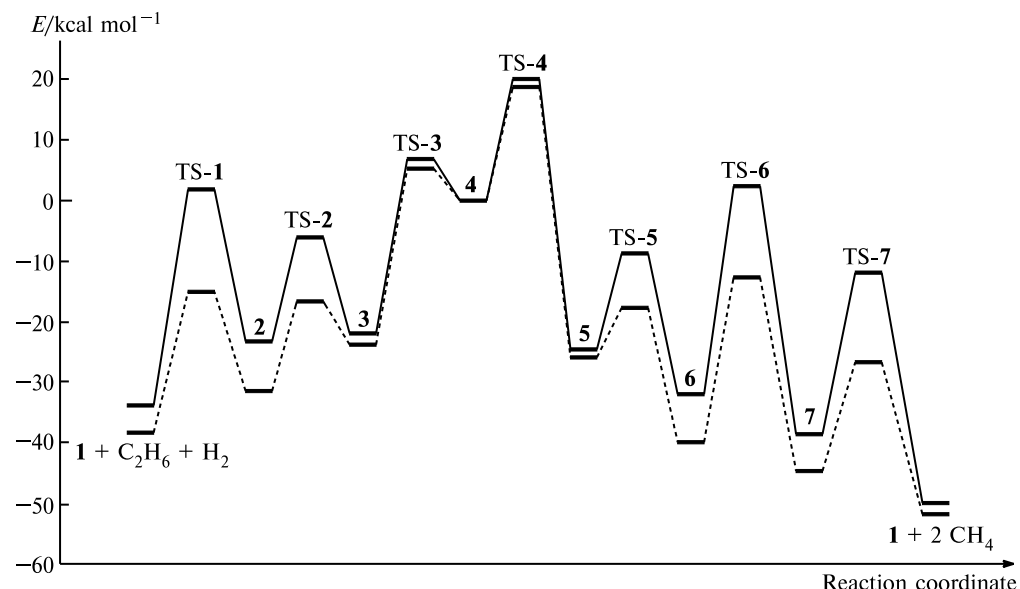
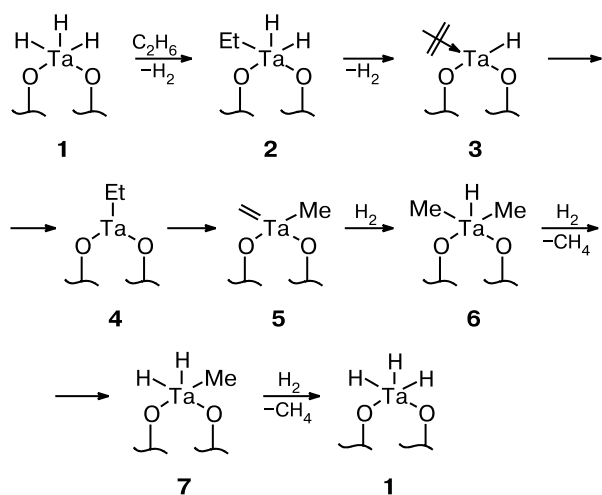


**Fig. 3.** Profile of the potential energy surface of ethane hydrogenolysis ( $\Delta E$  and  $\Delta G_{298}$  are indicated by dashed and solid lines, respectively). The structures of the clusters and transition states (TS) are shown in Scheme 2 and Fig. 2.

derivatives of energy with respect to coordinates. In addition, the intrinsic reaction coordinate (IRC) analysis of the reaction pathways was carried out for all transition states.<sup>23,24</sup> Since both methods gave very similar results, only the profile of the potential energy surface calculated at the B3LYP level is presented in Fig. 3.

**Scheme 2**



The first step of ethane hydrogenolysis (see Scheme 2 and Fig. 2) involves metathesis of the C—H bond proceeding through transition state TS-1 to form complex 2. Hydrogen elimination affords a complex with  $\eta^2$ -coordinated ethylene (3). The hydrogen transfer in the latter

complex gives rise to electron-deficient ( $q_{Ta} = 0.44$ ) Ta<sup>III</sup> complex 4. The subsequent cleavage of the C—C bond and the  $\beta$ -methyl transfer to the Ta atom afford Schrock-type carbene 5.<sup>25</sup> It appeared that in complex 5 in which the Ta atom is in a low oxidation state ( $q_{Ta} = 0.46$ ) and has a small number of d electrons, the carbene ligand has a high electron density ( $q_C = -0.21$ ). The subsequent interaction of hydrogen with Schrock-type complex 5 gives rise to complex 6 ( $q_{Ta} = 0.23$ ). In the course of addition at the Ta=C bond, hydrogen is much earlier bound to the Ta atom than to the C atom. In transition state TS-5 and equilibrium structure 6, the overlap populations of the Ta—H bond are 0.42 and 0.72, respectively, whereas these values for the C—H bond are 0.14 and 0.64, respectively. Analogously to the first step, the latter two steps of the process also involve  $\sigma$ -bond metathesis and proceed through four-center transition states TS-6 and TS-7 with regeneration of tantalum trihydride 1 and elimination of methane. Due to the relatively low activation barriers ( $\Delta G_{298}^{\ddagger} \approx 15\text{--}30\text{ kcal mol}^{-1}$ ), the catalytic cycle of ethane hydrogenolysis ( $\Delta G_{298} = -15\text{ kcal mol}^{-1}$ ) can be performed under the experimental conditions outlined (150 °C).<sup>17</sup>

To summarize, calculations of the reaction pathways demonstrate that ethane hydrogenolysis may proceed at a high rate according to the mechanism involving the formation of  $\pi$ -complexes and carbenium complexes of tantalum. The proposed catalytic cycle of ethane hydrogenolysis, which is constructed based on silica-supported tantalum trihydride, can be invoked to explain hydrogenolysis and metathesis of alkanes.

## References

- C. Lecuyer, F. Quignard, A. Choplin, D. Olivier, and J.-M. Basset, *Angew. Chem., Int. Ed.*, 1991, **30**, 1660.
- J. Corker, F. Lefebvre, C. Lecuyer, V. Dufaud, F. Quignard, A. Choplin, J. Evans, and J.-M. Basset, *Science*, 1996, **271**, 966.
- F. Quignard, C. Lecuyer, C. Bougault, F. Lefebvre, A. Choplin, D. Oliver, and J.-M. Basset, *Inorg. Chem.*, 1992, **31**, 928.
- L. d'Ornelas, S. Reyes, F. Quignard, A. Choplin, and J.-M. Basset, *Chem. Lett.*, 1993, 1931.
- R. Buffon, M. Leconte, A. Choplin, and J.-M. Basset, *J. Chem. Soc., Chem. Commun.*, 1993, 361.
- V. Dufaud, G. P. Niccolai, and J.-M. Basset, *J. Am. Chem. Soc.*, 1995, **117**, 4288.
- G. Niccolai and J.-M. Basset, *Appl. Catal. A*, 1996, **46**, 145.
- V. Vidal, A. Theolier, J. Thivolle-Cazat, J.-M. Basset, and J. Corker, *J. Am. Chem. Soc.*, 1996, **118**, 4595.
- V. Vidal, A. Theolier, J. Thivolle-Cazat, and J.-M. Basset, *Science*, 1997, **276**, 99.
- S. A. Holmes, F. Quignard, A. Choplin, R. Teissier, and J. Kervennal, *J. Catal.*, 1998, **176**, 173.
- S. A. Holmes, F. Quignard, A. Choplin, R. Teissier, and J. Kervennal, *J. Catal.*, 1998, **176**, 182.
- F. Lefebvre and J.-M. Basset, *J. Mol. Catal. A*, 1999, **146**, 3.
- O. Maury, L. Lefort, V. Vidal, J. Thivolle-Cazat, and J.-M. Basset, *Angew. Chem., Int. Ed.*, 1999, **38**, 1952.
- F. Lefebvre, J. Thivolle-Cazat, V. Dufaud, G. P. Niccolai, and J.-M. Basset, *Appl. Catal. A*, 1999, **182**, 1.
- J.-M. Basset, F. Lefebvre, and C. Santini, *Coord. Chem. Rev.*, 1998, **178–180**, 1703.
- O. Maury, L. Lefort, G. Saggio, C. Coperet, M. Taoufik, M. Chabanas, J. Thivolle-Cazat, and J.-M. Basset, *Stud. Surf. Sci. Catal.*, 2000, **130**, 917.
- M. Chabanas, V. Vidal, C. Coperet, and J.-M. Basset, *Angew. Chem., Int. Ed.*, 2000, **39**, 1962.
- W. J. Stevens, M. Krauss, H. Basch, and P. Jasien, *Can. J. Chem.*, 1992, **70**, 612.
- M. W. Schmidt, K. K. Baldridge, J. A. Boatz, S. T. Elbert, M. S. Gordon, J. J. Jensen, S. Koseki, N. Matsunaga, K. A. Nguyen, S. Su, T. L. Windus, M. Dupuis, and J. A. Montgomery, *J. Comput. Chem.*, 1993, **14**, 1347.
- N. D. Chuvylkin, *Zh. Fiz. Khim.*, 1983, **57**, 1129 [*J. Phys. Chem. USSR*, 1983, **57** (Engl. Transl.)].
- S. K. Ignatov, A. A. Bagatur'yants, A. G. Razuvaev, M. V. Alfimov, M. B. Molotovshchikova, and V. A. Dodonov, *Izv. Akad. Nauk, Ser. Khim.*, 1998, 1296 [*Russ. Chem. Bull.*, 1998, **47**, 1257 (Engl. Transl.)].
- M. N. Mikhailov, A. A. Bagatur'yants, and L. M. Kustov, *Izv. Akad. Nauk, Ser. Khim.*, 2003, 29 [*Russ. Chem. Bull., Int. Ed.*, 2003, **52**, 30].
- C. Gonzalez and H. B. Schlegel, *J. Chem. Phys.*, 1989, **90**, 2154.
- C. Gonzalez and H. B. Schlegel, *J. Phys. Chem.*, 1990, **94**, 5523.
- R. R. Schrock, *Acc. Chem. Res.*, 1979, **12**, 98.

Received May 23, 2003;  
in revised form June 11, 2003